Geoderma 455 (2025) 117202

Contents lists available at ScienceDirect

Geoderma

journal homepage: www.elsevier.com/locate/geoderma

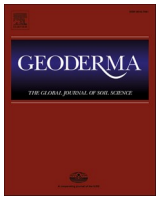

Deep-rooted perennials alter microbial respiration and chemical composition of carbon in density fractions along soil depth profiles

Kyungjin Min [a,b,c,*], Erin Nuccio [d,*], Eric Slessarev [d,e,f], Megan Kan [d], Karis J. McFarlane [d], Erik Oerter [d], Anna Jurusik [c], Gregg Sanford [g], Kurt D Thelen [h], Jennifer Pett-Ridge [c,d], Asmeret Asefaw Berhe [c]

[a] Department of Agricultural Biotechnology, Seoul National University, Seoul 08826, South Korea
[b] Research Institute of Agriculture and Life Sciences, Seoul National University, Seoul 08826, South Korea
[c] Department of Life and Environmental Sciences, University of California, Merced, CA 95343, USA
[d] Physical and Life Sciences Directorate, Lawrence Livermore National Laboratory, Livermore, CA 94550, USA
[e] Department of Ecology and Evolutionary Biology, Yale University, New Haven, CT 06511, USA
[f] Yale Center for Natural Carbon Capture, Yale University, New Haven, CT 06511, USA
[g] Department of Soil and Environmental Sciences, University of Wisconsin – Madison, Madison, WI 53706, USA
[h] Department of Plant, Soil & Microbial Sciences, Michigan State University, East Lansing, MI 48824, USA

ARTICLE INFO

Handling Editor: C. Rumpel

Keywords:
Density fraction
^{14}C
Mid-infrared spectroscopy
DRIFT
Deep soil
Root

ABSTRACT

Growing deep-rooted perennials has been proposed to increase soil organic carbon (SOC) stocks and mitigate CO_2 emissions. Yet, we know little about the bioavailability and chemical properties of SOC under deep-rooted perennials and shallow-rooted annuals. Improving our understanding of the role of deep-rooted perennials for belowground C storage is critical, as root growth has the potential to both increase SOC stock and accelerate loss of existing SOC. Here, we assessed the effects of >10 years of land conversion from shallow-rooted annuals (maize) to deep-rooted perennials (switchgrass) on SOC bioavailability (microbial respiration, $\Delta^{14}C\text{-}CO_2$), mineral-associated SOC (density fractionation), and SOC turnover and composition (^{14}C-SOC, DRIFT spectroscopy) in surface soils (0–20 cm) and subsoils (90–120 cm) at two sites with sandy and silty soils. We demonstrate that switchgrass enhanced microbial respiration of recently-fixed C in surface soils. Switchgrass increased $\Delta^{14}C$ values of the free light fraction in subsoil of the sandy site, by supplying aliphatic C (putative simple plant C) into the soil. In contrast, maize input less root C into the soil, and at one site increased the decomposition of older SOC, which indicates that overall microbial C demand outpaced plant C inputs. These results highlight that deep-rooted perennials stimulate the transfer of more atmospheric C to both surface and subsoils than shallow-rooted annuals, that newly generated SOC under deep-rooted perennials is relatively less protected from decomposition, and that reaping the C benefits of deep-rooted perennials could require maintaining the land cover as a perennial cropping system.

1. Introduction

More than 116 Pg C has been lost from soil to the atmosphere since the onset of agriculture (Sanderman et al., 2017, 2018). Restoring a fraction of this lost C would help to sequester atmospheric carbon dioxide and mitigate climate change (Lal, 2004). Growing deep-rooted plants, especially perennials, in agricultural land is one potential strategy for enhancing soil organic carbon (SOC) sequestration (Lorenz and Lal, 2005; Kell, 2011, 2012; Paustian et al., 2016; Button et al., 2022; Longbottom et al., 2022). This approach takes advantage of deep soil that is not at its C storage capacity (Schiedung et al., 2019) and the relatively high transformation efficiency of root-derived C to SOC (Rasse et al., 2005; Sokol and Bradford, 2019). While some studies report increases in SOC contents and stocks after land conversion from shallow- to deep-rooted plants (Fisher et al., 1994; Conant et al., 2017; Slessarev et al., 2020), limited data exists on the distribution of sequestered C in fractions or along the soil profile, its chemical or isotopic composition, and relations to microbial processing at depth. These properties can

* Corresponding authors at: Department of Agricultural Biotechnology, Seoul National University, Seoul 08826, South Korea (K. Min).
E-mail addresses: kjmin@snu.ac.kr (K. Min), nuccio1@llnl.gov (E. Nuccio).

https://doi.org/10.1016/j.geoderma.2025.117202
Received 23 September 2024; Received in revised form 11 January 2025; Accepted 3 February 2025

indicate whether SOC stored under deep-rooted plants is more or less likely to be vulnerable to environmental changes and persist long enough as a carbon dioxide removal strategy.

Roots can alter the amount of soil organic matter physically associated with minerals and its chemical and isotopic composition. For instance, root growth can accelerate the turnover of root biomass (Eshel and Beeckman, 2013), which tends to accumulate as low-density particulates that are not strongly associated with minerals (free light fraction; fLF). If this occurs, fLF can become enriched in compounds such as lignin and suberin and, consequently, in ^{14}C. Despite their derivation from recently assimilated C, these compounds are often slower to decompose than older soil organic matter (Riederer et al., 1993; Spielvogel et al., 2010). In addition to contributing senesced biomass, roots can produce exudates that stimulate microbial growth and associated metabolite secretions (Zhalnina et al., 2018; Pett-Ridge et al., 2020). Microbial biomass and byproducts can enhance occlusion, adhesion, and sorption of organic matter to mineral surfaces, increasing the amount of C trapped inside of mineral aggregates (commonly quantified as the occluded light fraction; oLF) and physically bound to mineral particles (heavy fraction; HF) (Sokol et al., 2022). Alternatively, root exudates may liberate mineral-bound OC by stimulating microbial activity or directly destabilizing organo-mineral associations; this outcome is termed the "priming effect" (Keiluweit et al., 2015; Shahzad et al., 2018). As Dijkstra et al. (2021) pointed out, roots can serve as a "double-edged sword", either increasing SOC via microbial necromass formation, organo-mineral complexation, and aggregate formation, or decreasing SOC via accelerated decomposition of old C, organo-mineral decomplexation, and aggregate destruction. The balance of processes that increase or decrease SOC ultimately impacts total SOC content.

Investigating the composition and ^{14}C of SOC can help us assess processes through which plants and microbes influence the formation of SOC. While the ultimate source of C in the soil is largely plant-derived, microbial assimilation of C into biomass and, eventually, necromass can also leave a fingerprint on SOC. For example, Waksman (1925) reported that microbially-derived proteins constitute a significant portion of SOC. More recent studies estimate that microbial products comprise as much as 50 % of the mineral associated SOC pool (Angst et al. 2021). Employing mid-infrared spectroscopy and extensive literature search, Mainka et al. (2022) recently compiled common SOC functional groups and their origins: aliphatic (C–H stretch, mostly from plant litter or root exudates as in organic acids; hereafter simple plant C), aromatic (C═C stretch, mostly from lignin or phenolic root exudates; hereafter complex plant C), and amide/quinone/ketone/aromatic/carboxylate (C═O, C═C, and C–O stretch, mostly from microbial cell walls and membrane lipids; hereafter microbial C). This approach can be useful in studying plant and microbial processes that shape SOC. If roots provide soil with border cells (previously sloughed cells), the abundance of aliphatic (suberin, wax) and aromatic (lignin) functional groups can increase (Franke and Schreiber, 2007; Eshel and Beeckman, 2013; Vranova et al., 2013; Williams and de Vries, 2020) as well as increases in ^{14}C signal (Angst et al., 2016). If root exudates (e.g., acetic, citric, oxalic, succinic acids) are released into the soil and escape from microbial utilization, aliphatic functional groups (organic acid root exudates) may increase. Alternatively, if microbial communities use up most of the root exudates for growth, amide/quinone/ketone/aromatic/carboxylate functional groups (microbial cell walls and membrane lipids) may increase. As such, the relative abundance of simple plant C (aliphatic) to microbial C (amide/quinone/ketone/aromatic/carboxylate) may hint on SOC dynamics: the lower the ratio is, the greater microbial utilization is. When root exudates prime the loss of mineral-associated OC, we may detect decreases in microbial C in the HF because microbial necromass accumulates on the mineral surface (Miltner et al., 2012).

Here, we investigate the effects of land conversion from shallow-rooted annuals to deep-rooted perennials on the physical, chemical, and biological properties of SOC at two study sites with contrasting soil textures. These sites were part of a larger national-scale sampling campaign that examined SOC under switchgrass plantings and neighboring row crops; they were selected for these more intensive analyses because they featured well-documented experimental designs. We used density fractionation, Diffuse Reflectance Infrared Fourier Transform Spectroscopy (DRIFT), and $\Delta^{14}C$ of microbial respiration and SOC in density fractions to closely assess any changes in elemental (%OC), isotopic, and spectroscopic properties of SOC under shallow vs. deep-rooted plants. We hypothesized that: 1) deep-rooted perennials will increase the rate and $\Delta^{14}C$-CO_2 values of microbial respiration in deep soils, 2) deep-rooted perennials will increase the relative mass and OC of fLF and oLF, and 3) deep-rooted perennials will increase the ratio of complex C to microbial C and $\Delta^{14}C$-SOC in each fraction.

2. Materials and methods

2.1. Study sites

We chose two study sites where both deep-rooted perennials (switchgrass) and shallow-rooted annuals (continuous maize) have been growing for more than ten years. All the soil and root samples were collected in June 2019. Note that maize was not at its peak biomass in June, so there is a possibility that we underestimated dry root biomass for maize. The first site was the GLBRC Biofuel Cropping System Experiment at the Kellogg Biological Station in Hickory Corners, MI (hereafter sandy site). At this site, the mean daily maximum/minimum temperatures are 14.6/4.4 °C, with annual precipitation of 897.64 mm in 2019 (mawn.geo.msu.edu/station.asp?id=kbs&rt=24). The soils are dominated by the Kalamazoo series (Fine-loamy, mixed, active, mesic, Typic, Hapludalfs, Web Soil Survey). The sandy site was established in 2008 as a randomized complete block design with five replicated blocks and ten treatments (total 50 plots = 10 treatment plots per block × 5 blocks). Each plot is 30 × 40 m, separated by 15 m in between plots. Among the 50 plots, we selected six plots for soil and root sampling, three for continuous maize (*Zea mays L.*) and three for switchgrass (*Panicum virgatum*, Cave-in-Rock). Maize plots were managed as a no-till system and were sprayed with herbicide as necessary for weed control (usually 2 times a year). Maize was planted in May and received straight fertilizers (170 kg-N ha^{-1} yr^{-1}, 67 kg-P ha^{-1} yr^{-1}, 84 kg-K ha^{-1} yr^{-1}). Grain from maize was machine-harvested in October. Remaining aboveground Maize stover residue was machine-harvested (baled) between October and November. Switchgrass plots received no fertilizer. Since plot establishment, the aboveground switchgrass biomass has been annually machine-harvested post-senescence during October and November. None of the plots were treated with cover crops.

The second site was the Wisconsin Integrated Cropping Systems Trial (WICST) at the Arlington Agriculture Research Station in Arlington, WI (hereafter silty site). In 2019, the mean daily maximum/minimum temperatures were 12.1/1.1 °C. The site received annual precipitation of 1160.76 mm (mawn.geo.msu.edu/station.asp?id=alt&rt=24). The soils are classified as Plano silt loam (Fine-silty, mixed, superactive, mesic, Typic, Argiudolls). Continuous maize at the silty site was established in 1990 as part of the core WICST trial, a large-scale (24 ha) randomized complete block design with four blocks (Each maize plot = 18 × 155 m). Switchgrass plots at the silty site were established in the nested "prairie" experiment in 2007. This nested experiment is also laid out in a randomized complete block design with three blocks. Prior to planting switchgrass in 2007, continuous maize had been grown at the site since 1999, consistent with the core WISCT trail. Switchgrass plots (experimental units) are 4 × 20 m. We collected samples from three continuous maize and three switchgrass (*Panicum virgatum*, Forestberg) plots. Maize was planted in May and received fertilizers at 112 kg ha^{-1} yr^{-1} in May (NPK fertilizer) and at 180 kg ha^{-1} yr^{-1} in June (N fertilizer). The maize plots were sprayed with pesticides and herbicides when necessary. No cover crops were planted in the maize plots. Grain was harvested in October and November. Soils were tilled after harvest in November and before planting in May. The switchgrass plots were treated with

pesticides before and after emergence, but did not receive fertilizer. The aboveground biomass of switchgrass was harvested once a year in October.

2.2. Soil sampling and SOC

At each selected plot (total of 12 plots), we collected soils using a Geoprobe 54LT hydraulic drilling machine (Geoprobe, Salina, USA) in June 2019. We used MC5 tooling (Ø = 3.175 cm) for one plot at the sandy site but had to switch to MC7 (Ø = 7.62 cm) for the remaining 11 plots to avoid compaction of soil in the core and associated changes in the depth interval. The sampling depth was 240 cm, and we divided the soil cores into nine depth intervals, including 0–20, 20–40, 40–60, 60–90, 90–120, 120–150, 150–180, 180–210, and 210–240 cm. We measured soil weight for each depth interval, before and after picking out roots and rocks in order to estimate bulk density. We shipped samples in a 4 °C cooler to the Lawrence Livermore National Laboratory. Fresh soil was used for incubation and CO_2 measurement, while air-dried and 2 mm sieved soils were used for density fractionation (check below). We also picked out root fragments after 2 mm sieving. Root biomass was measured after rinsing and drying roots at room temperature. Soil pH was measured in a 1:2 = soil:water (w/v) solution (Hanna HI5522, Italy). When the soil pH was greater than 6.5, samples were acid-treated with 1 M HCl to remove inorganic C due to carbonates. All samples were sent to UC Berkeley for $\delta^{13}C$ measurements (acid treated and untreated) using an EA-IRMS (CHNOS Elemental Analyzer interfaced to an IsoPrime100 mass spectrometer). All non-acid treated samples were also sent to Oregon State University Soil Health Lab for total CN (Elementar Vario Macro Cube) (Fig. S1).

2.3. Incubation of soils, CO_2 respiration rate, and $\Delta^{14}C$-CO_2

We chose two soil depth intervals (0–20 and 90–120 cm) for the measurements of CO_2 respiration rate, $\Delta^{14}C$-CO_2, density fractionation, and $\Delta^{14}C$-SOC in density fractions (total 24 samples = 2 depth intervals × 2 vegetation × 3 replicates × 2 study sites). We used 100–120 g of fresh soil from each depth interval depending on the sample availability and our initial estimate of the coarse fragments content. That is, we used more fresh soil when we expected a significant portion of soil to be >2 mm. We placed soil in quart (946 mL) canning jars, and initiated the soil incubations four weeks after sample collection in the field, to allow time for residual live roots to stop respiring and to allow for water-content adjustment. Jars were stored in the dark at room temperature (approximately 20 °C) throughout the incubation. Before the start of respiration measurements, each fresh soil sample was wetted (if too dry) or air-dried (if too wet) to 60 % of its water-holding capacity and maintained in a sealed jar for 1 week. We did this because maintaining 50–60 % of water-holding capacity is ideal for measuring microbial respiration during incubation (Franzluebbers, 1999). After this resting period, soil respiration was quantified by periodically sampling the jar headspace through a rubber septum with a 1 mL syringe and measuring the CO_2 concentration with a Li840 Infrared Gas Analyzer (LiCOR, Lincoln, NE, USA). We estimated average respiration rates over the first two weeks of the incubation by regressing the moles of CO_2 in each jar against time, extracting the slope coefficient (moles $time^{-1}$), and dividing by the dry mass of soil in the jar (CO_2 accumulation rates were approximately linear during the initial phase of the incubation)(μg C g^{-1} day^{-1}). After this initial two-week period, we checked the CO_2 concentration in each jar periodically and extracted CO_2 for ^{14}C analysis after each jar reached a CO_2 partial pressure of at least 10,000 ppm. The incubation time varied with samples to allow sufficient CO_2 accumulation for $\Delta^{14}C$-CO_2 analysis. For example, soils at 0–20 cm took 14–30 days to reach 10,000 ppm of CO_2, while soils at 90–120 cm required up to 183 days to accumulate sufficient CO_2 for the $\Delta^{14}C$-CO_2 analysis.

2.4. Density fractionation

For density fraction analysis, we used three to five analytical replicates per sample (total 24 samples = 2 depth intervals × 2 vegetation × 3 replicates × 2 study sites). For ^{14}C analysis, we composited these analytical replicates to obtain sufficient sample mass. We modified the density fractionation method described in Swanston et al. (2005). Briefly, we added 75 mL of 1.65 g cm^{-3} of sodium polytungstate (TC-Tungsten compounds, Augsburg, Germany) to 20 g of air-dried, 2 mm sieved soil. After letting the mixture sit at room temperature for 45 min, we centrifuged the samples at 2,684 × *g* at 4 °C for 45 min. The free light fraction (fLF), which is the material that remained floating after centrifugation, was aspirated into a pre-labeled flask and filtered through a pre-dried at 450 °C and pre-weighed 0.7 μm glass fiber filters (AP4004705, 47 mm, Millipore, Ireland). The fLF on the filter was rinsed with ultrapure water five times and dried at 55 °C for 2 d. The remaining mixture was further mixed at 1,700 min^{-1} (IKA©RW20 digital) for 1 min and sonicated in ice at 200 J mL^{-1} for 3 min (Branson Digital Sonifer 450). After sitting the mixture at room temperature for 45 min, we centrifuged the samples at 2,684 × *g* at 4 °C for 45 min. The supernatant, occluded light fraction (oLF), was aspirated into a pre-labeled flask and filtered through a pre-dried at 450 °C and pre-weighed 0.7 μm GF/F filters (AP4004705, 47 mm, Millipore, Ireland). The oLF on the filter was rinsed with ultrapure water five times and dried at 55 °C for 2 d. We added 150 mL of DI into the pelleted, heavy fraction (HF), vortexed to mix, centrifuged at 2,684 × *g* at 4 °C for 45 min, and aspirated out the DI. We repeated this procedure two more times to completely remove sodium polytungstate solution (for the last repetition, we centrifuged the samples at 3,314 × *g* for 1 h). The pelleted HF was collected into a pre-weighed aluminum dish and dried at 105 °C for 2 d.

Fractionated samples were ground to a powder (8000 M, SPEX SamplePrep, USA) and analyzed for total OC, ^{14}C, DRIFT, and via scanning electron microscopy (Fig. S2). Note that we ground fLF and oLF along with the glass fiber filters and later corrected total OC content using the dilution factor (sample weight: filter weight). In a preliminary experiment, ground glass fiber filters did not alter the spectrum of DRIFT at the range of 4,000–400 cm^{-1}. Overall, the average mass recovery after density fractionation was 98.0 ± 1.4 % and the average OC recovery was 92.4 ± 14.3 % after correcting for the loss of mass during density fractionation. The proportion of OC in each fraction to the bulk SOC was also expressed after taking the loss of mass into account.

2.5. Diffuse Reflectance Infrared Fourier Transform Spectroscopy (DRIFT)

DRIFT was performed on the bulk and density fractionated soils at 0–20 and 90–120 cm. Before DRIFT measurements, soil samples were finely ground and oven-dried at 60 °C overnight (Min and Choi 2022). Diffuse reflectance absorbance (=−log reflectance) was measured between 4,000 and 400 cm^{-1}, and averaged over 32 scans (ALPHA-II, Bruker, USA). The absorbance at the wavenumbers of 2976–2898 and 2870–2839 cm^{-1} indicates aliphatic C–H stretch from plant litter and organic acid root exudates (Ellerbrock and Gerke, 2004; Vranova et al., 2013; Mainka et al., 2022) (putative simple plant C). The peaks between 1550 and 1500 cm^{-1} are due to aromatic C═C stretch from lignin or aromatic root exudates (putative complex plant C). The peaks at 1660–1580 cm^{-1} represent amide/quinone/ketone (C═O) stretch, aromatic (C═C) stretch, or carboxylate (C–O) stretch (mostly from microbial cell walls, lipids)(putative microbial C). Often, a low ratio of simple plant C to microbial C indicates microbial transformation of plant-derived C to microbial biomass, and a high ratio of complex plant C to microbial C suggests a relatively high supply of complex plant C to soil (Ryals et al., 2014; Mainka et al., 2022).

2.6. $\Delta^{14}C$ of density fractionated soils

Radiocarbon values were assessed on density fractions from 0 to 20 and 90 to 120 cm depths at the Center for Accelerator Mass Spectrometry (AMS) at Lawrence Livermore National Laboratory (NEC 1.0 MV Tandem or the FN Tandem Van de Graaff AMS) (Broek et al., 2021). Samples were combusted to CO_2 in the presence of Ag and CuO and reduced onto Fe powder in the presence of H_2. Aliquots of CO_2 were analyzed for ^{13}C at the Department of Geological Sciences Stable Isotope Laboratory, University of California Davis (GVI Optima Stable Isotope Ratio Mass Spectrometer). The ^{14}C content of each sample was reported in $\Delta^{14}C$ notation, corrected for mass-dependent fractionation with measured $\delta^{13}C$ values, and then corrected to the year of measurement for ^{14}C decay since 1950 (Stuiver and Polach, 1977).

2.7. Statistical analyses

We compared root biomass between switchgrass and maize along soil depth profiles. We set up a mixed-effects model for each site, with vegetation type and depth as fixed effects, soil core as a random effect, and root biomass as a dependent variable. We used *lme* (linear mixed effects) function and restricted maximum likelihood method for post-hoc analyses in the nlme package (R core team 2024). For microbial respiration ($[CO_2]$ and $\Delta^{14}C\text{-}CO_2$) and chemical properties (OC, DRIFT and $\Delta^{14}C$) of density fractions, we used a two-way ANOVA at a given depth interval, with vegetation type and site as explanatory variables. The Tukey method was used to as a post-hoc comparison. We considered model terms to be statistically significant if the p value for a null model without the term was less than or equal to the threshold $\alpha = 0.05$.

3. Results

3.1. Root biomass

We quantified root biomass captured in soil cores at each depth interval (Fig. 1). Switchgrass roots were deeper and more abundant at 0–40 cm than maize roots at both sites ($p < 0.001$ for both sites). The rooting depth of switchgrass was 0–210 cm at the sandy site (Fig. 1.a) and 0–150 cm at the silty site (Fig. 1.b). Below 60 cm, we were not able to find maize roots in any of the soil cores.

3.2. Microbial respiration in top vs. subsoil layers

We focused additional laboratory experimental analyses on two depth intervals, 0–20 cm and 90–120 cm, to investigate microbial respiration ($[CO_2]$ and $\Delta^{14}C\text{-}CO_2$) and chemical properties (OC, DRIFT and $\Delta^{14}C$) of density fractions. We reasoned that the root effects on microbial respiration and chemical properties of SOC would be pronounced at 0–20 cm due to the large difference in root biomass between switchgrass and maize, and below the rooting zone of maize but within the rooting zone of switchgrass at 90–120 cm.

At 0–20 cm, microbial respiration was greater in soils under switchgrass than those under maize ($p = 0.042$; Fig. 2.a). When we pooled microbial respiration data from 0-20 cm across both sites, the mean respiration rate under switchgrass was 6.51 μg $C\text{-}CO_2$ g^{-1} h^{-1}, 1.7 times greater than that under maize (Fig. 2.a). In contrast, microbial respiration from 90–120 cm soils was similar between switchgrass and maize at both sites (Fig. 2.b). Values of $\Delta^{14}C\text{-}CO_2$ were significantly influenced by the interaction between vegetation type and site at 0–20 cm ($p < 0.001$; Fig. 2.c). $\Delta^{14}C\text{-}CO_2$ was lower (i.e., older) under maize at the sandy site ($p = 0.002$), while the values of $\Delta^{14}C\text{-}CO_2$ were not significantly different between switchgrass and maize at the silty site. At 90–120 cm, we did not find significant effects of vegetation type or site on the values of $\Delta^{14}C\text{-}CO_2$ (Fig. 2.d).

3.3. Elemental, microscopic, spectroscopic, and isotopic properties of SOC of density fractions

To determine how vegetation type influenced SOC chemistry, we density fractionated soils collected from 0 to 20 cm and 90 to 120 cm and assessed the elemental (%OC), microscopic, spectroscopic, and isotopic properties of OC in each fraction. Each density fraction exhibited different percent OC content, with fLF and oLF being high compared to HF (Table 1). The proportion of OC in each fraction relative to the bulk SOC did not vary with vegetation type at 0–20 cm (Fig. 3, left). In contrast, the proportion of OC in the fLF at 90–120 cm seemed to vary with the interaction between vegetation type and site ($p = 0.062$; Fig. 3.b). Specifically, at the sandy site, the proportion of OC in the fLF was greater in soils under switchgrass ($p = 0.057$), while the proportion of OC in the fLF was similar between switchgrass and maize at the silty site.

We visually investigated a portion of density fractions (samples at 0–20 cm at the sandy site) under scanning electron microscopy to check if distinct SOC pools were separated by density fractionation (Fig. S2). Morphologies of fLF and oLF were visually distinct from those of HF and morphologies were similar between switchgrass and maize for a given fraction. In line with this microscopy data (Fig. S2), each density fraction exhibited a distinct DRIFT spectrum (Fig. 4, Table 2, Figs. S3–S5):

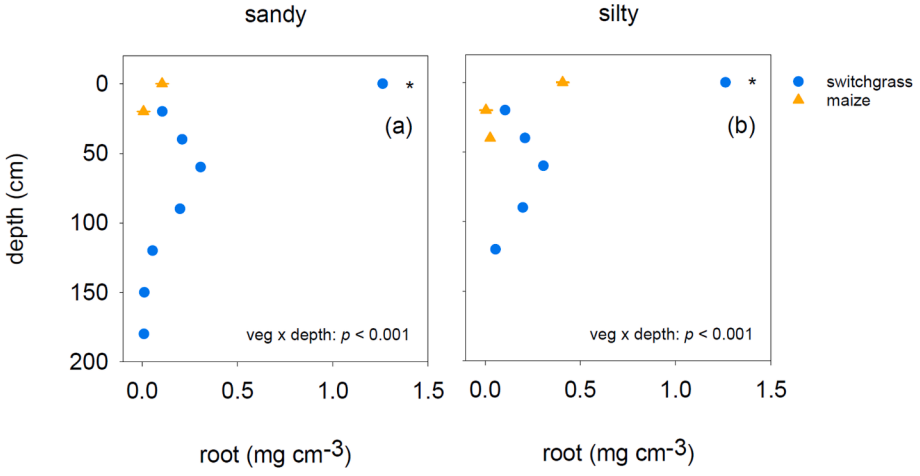

Fig. 1. Root distribution along soil depth profiles (0–240 cm) collected in June 2019 from two contrasting cropland sites planted with switchgrass (blue) or maize (orange) grown at the sandy (a, Kellogg Biological Station, MI) and silty (b, Arlington Agriculture Research Station, WI) sites. N = 3 per crop type and location. Mean + standard deviation.

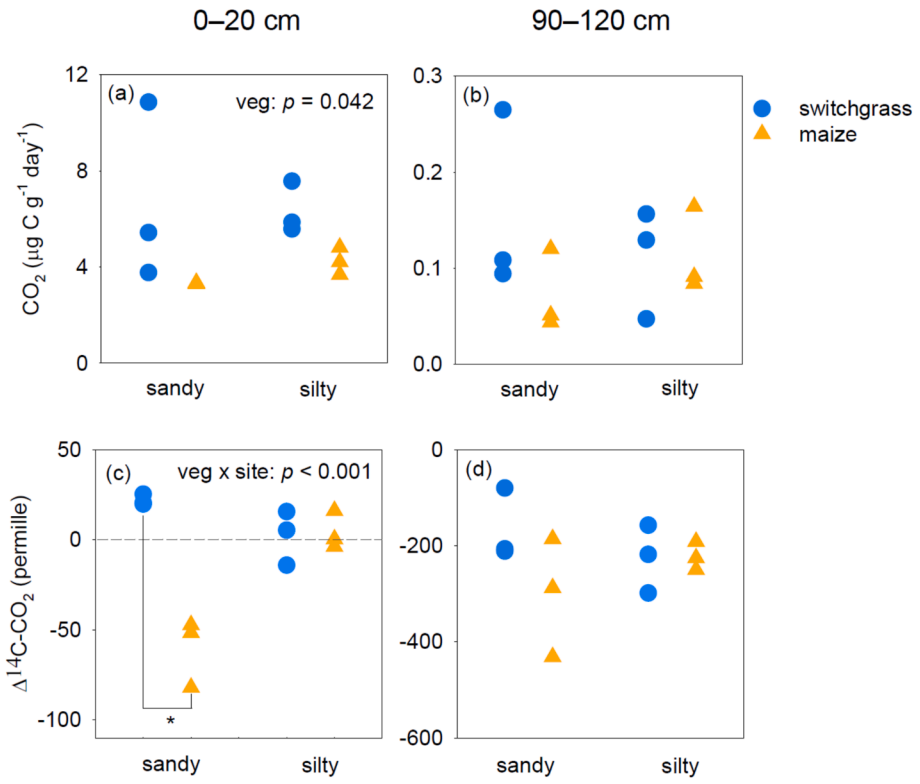

Fig. 2. The rates (a and b) and $\Delta^{14}C$ (c and d) of microbial respiration from soils collected in June 2019 from two contrasting cropland sites planted with switchgrass (blue) or maize (orange) grown at the sandy (Kellogg Biological Station, MI) and silty (Arlington Agriculture Research Station) at depth intervals of 0–20 and 90–120 cm (N = 3). Note the different scales on the y-axes. Dotted line represents modern C. Asterisk was drawn to show a significant difference at $p < 0.05$.

Table 1
Percent organic carbon in bulk soil and density fraction, and the relative mass of each fraction to the bulk soil mass under switchgrass and maize at 0–20 cm and 90–120 cm at the sandy and silty sites. Mean (Standard error). Lower case letters represent a significant difference in percent OC between switchgrass and maize at a given site, depth, and fraction at α = 0.05, while upper case letters indicate a significant difference in percent OC among fractions at a given site, depth, and vegetation at α = 0.05.

Site	Depth (cm)	Vegetation	Bulk SOC(%)	Percent OC in each fraction(%)			Relative mass of each fraction to the bulk soil mass (%)		
				fLF	oLF	HF	fLF	oLF	HF
Sandy	0–20	Switchgrass	0.90(0.10)	8.89^{A}(2.05)	9.22 ^{A}(0.63)	0.51^{B}(0.02)	0.95 (0.29)	2.03 (0.38)	97.02 (0.64)
		Maize	0.73(0.09)	5.91^{B}(0.43)	9.05 ^{A}(1.05)	0.32^{C}(0.08)	0.63 (0.06)	1.30 (0.36)	98.07 (0.38)
	90–120	Switchgrass	0.06(0.01)	1.06^{Aa*}(0.26)	0.90^{A}(0.32)	0.04^{B}(0.002)	0.20 (0.06)	0.03 (0.00)	99.77 (0.06)
		Maize	0.08(0.01)	0.55^{Ab*}(0.04)	0.67^{A}(0.21)	0.05^{B}(0.01)	0.16 (0.06)	0.18 (0.14)	99.66 (0.18)
Silty	0–20	Switchgrass	2.06(0.19)	7.15^{A}(0.80)	9.17 ^{A}(0.80)	1.25^{B}(0.15)	1.01 (0.24)	4.34 (0.49)	94.65 (0.49)
		Maize	2.22(0.18)	6.32^{B}(0.50)	8.25 ^{A}(0.81)	1.31^{C}(0.22)	1.23 (0.16)	4.68 (0.27)	94.09 (0.43)
	90–120	Switchgrass	0.18(0.004)	0.73(0.02)	1.02(0.36)	0.17(0.01)	0.10 (0.03)	1.18 (0.79)	98.72 (0.76)
		Maize	0.16(0.006)	0.67(0.07)	1.54(0.60)	0.14(0.01)	0.09 (0.03)	0.39 (0.22)	99.52 (0.20)

*$p = 0.057$.

The fLF contained a relatively high abundance of all functional groups that we examined in this study: putative simple plant C, complex plant C, and microbial C. The oLF also included all types of functional groups, with microbial C more abundant than in the fLF. In contrast, HF contained little simple and complex plant C, but was dominated by microbial C. Also, the HF contained several peaks at 2,000–1,800 cm^{-1}, which are characteristic of quartz.

We calculated the ratio of simple plant C to microbial C, and the ratio of complex plant C to microbial C (Fig. 5 and 6, Table S1). The former suggests the degree of microbial transformation of aliphatic, simple plant C into microbial biomass/necromass, and the latter reflects the supply of aromatic, complex plant C to the soil relative to microbial growth (Ryals et al., 2014; Mainka et al., 2022). In our samples, there was no significant vegetation effect on the ratio of simple plant C to microbial C in bulk soil (Table S1) nor in any of the density fractions at 0–20 cm (Fig. 5, left). In contrast, the fLF ratio of simple plant C to microbial C was greater for switchgrass than maize at 90–120 cm, especially at the sandy site ($p = 0.039$; Fig. 5.b). This was primarily due to the increases in simple plant C, not the decreases in the microbial C (Table 2). The interaction between vegetation type and site significantly influenced the ratio of complex plant C microbial C in oLF at 0–20 cm ($p = 0.049$; Fig. 6).

Vegetation type significantly influenced $\Delta^{14}C$ of the fLF at 90–120 cm ($p = 0.025$); the $\Delta^{14}C$ values of the fLF were greater in switchgrass relative to maize soils (Fig. 7.b). We did not observe any vegetation effect on the values of $\Delta^{14}C$ in other fractions or at 0–20 cm. Contrary to distinct microscopy pictures and DRIFT spectrum among density fractions (Figs. S2–S4, Fig. 4), $\Delta^{14}C$ of density fractions overlapped at all depth intervals (Fig. 7).

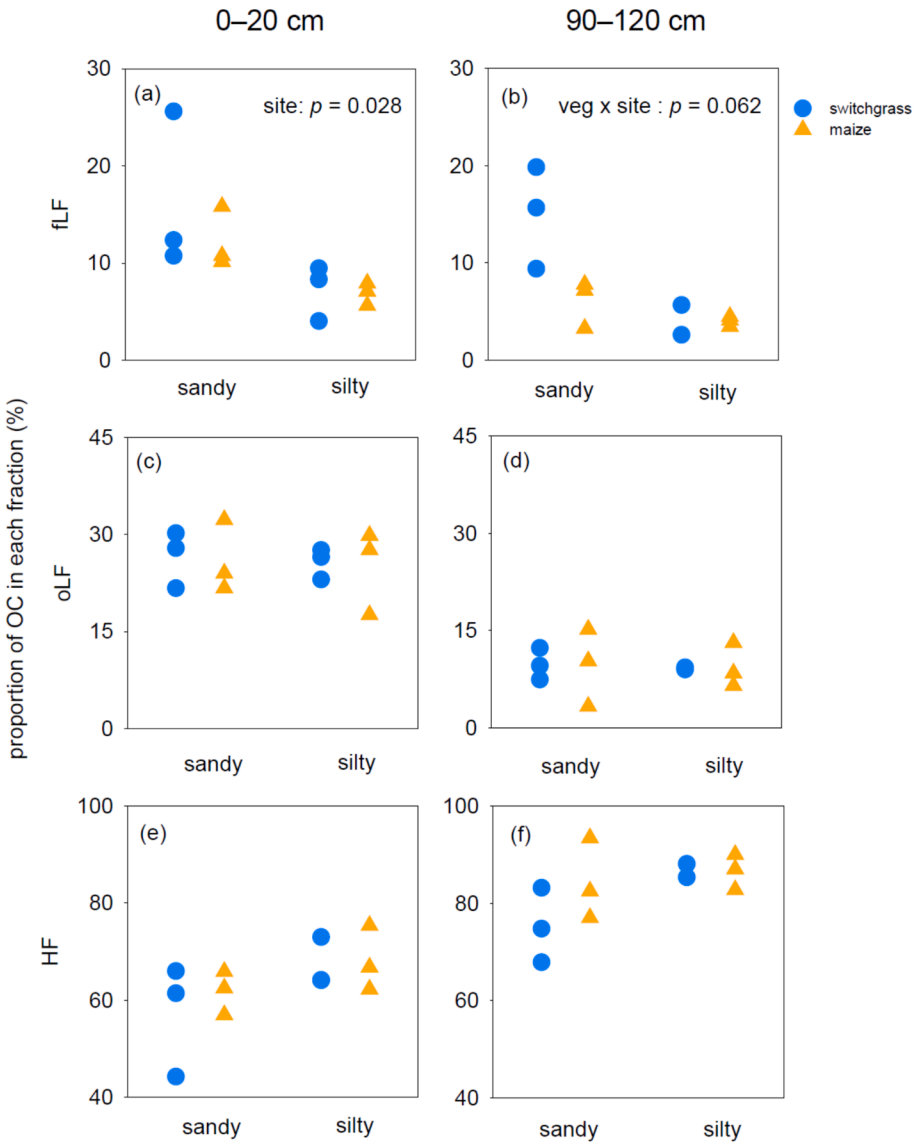

Fig. 3. Proportion of OC in each fraction to the bulk SOC from soils collected in June 2019 from two contrasting cropland sites planted with switchgrass (blue) or maize (orange) grown at the sandy (Kellogg Biological Station, MI) and silty (Arlington Agriculture Research Station) at depth intervals of 0–20 and 90–120 cm (N = 3). fLF, free light fraction (a and b); oLF, occluded light fraction (c and d); HF, heavy fraction (e and f). The proportion of OC (%) was calculated by taking the loss during density fractionation into account (sum = 100%).

4. Discussion

We designed this study to test the effects of shallow-rooted annuals (maize) vs. deep-rooted perennials (switchgrass) on the physical, chemical, and biological properties of soil organic carbon at two study sites with contrasting soil textures. In addition to increasing plant root inputs, we demonstrate that switchgrass enhanced microbial respiration and use of plant-derived C in shallow soil layers. In deep soil layers, switchgrass increased the relative abundance of SOC and $\Delta^{14}C$ values of free light fraction, by increasing the input of aliphatic C (putative simple plant C) into the soil C pool.

4.1. Deep-rooted perennials promote the use of plant-derived C by microbes in shallow soil layers

Contrary to our first hypothesis that deep-rooted perennials will increase the rate and $\Delta^{14}C$-CO_2 values of microbial respiration in deep soil layers, we observed a significant difference in microbial respiration and $\Delta^{14}C$-CO_2 in surface soils (at 0–20 cm), but not at 90–120 cm (Fig. 2). This suggests that root abundance, more than merely the presence of roots, influenced microbial activity (Figs. 1 and 2). This pattern would be expected if root exudation and production of rhizodeposits scale roughly with root biomass or if mass-specific root inputs decline with depth. Tückmantel et al. (2017) showed that total root exudation decreases with soil depth due to decreasing root mass-specific exudation in a beech forest. Similarly, using ^{13}C labeling, Peixoto et al. (2020) demonstrated that rhizodeposition from perennial deep-rooted plants decreased with depth. The amount of C that is lost via root exudation and rhizodeposits is estimated as high as 5–21 % of the total fixed C (Haichar et al., 2014; Driouich et al., 2013; Eshel and Beeckman, 2013). The types of C include carbohydrates (glucose, sucrose, polysaccharide), amino acids, organic acids (oxalic acid, citric acid, malic acid), and lipids (Miao et al., 2020; Baker et al., 2024). Assuming similar patterns in our study system, plant root exudates and rhizodeposits were likely highest at 0–20 cm among the depth intervals due to the greater root biomass near the surface (Fig. 1) and presumably the greatest root mass-specific exudation. Indeed, the abundance of aliphatic compounds, which could be derived from relatively simple plant C, was higher at

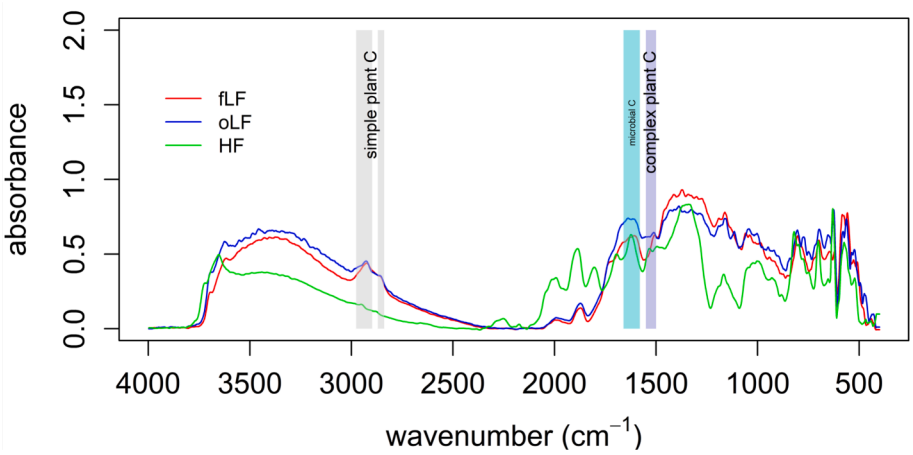

Fig. 4. Example mid-infrared Diffuse Reflectance Infrared Spectroscopy spectrum for one soil sample at 0–20 cm under switchgrass at the sandy site (Kellogg Biological Station, MI) (fLF, free light fraction; oLF, occluded light fraction; HF, heavy fraction). Peaks at 2976–2898 and 2870–2839 cm^{-1} represent aliphatic (C–H stretch; putative simple plant C), 1550–1500 cm^{-1} for aromatic (C═C stretch; putative complex plant C), and 1660–1580 cm^{-1} for amide/quinone/ketone (C═O stretch), aromatic (C═C stretch), and carboxylate (C–O stretch)(putative microbial C) groups.

Table 2
Peak area of Diffuse Reflectance Infrared Fourier Transform (DRIFT) spectra collected from the free light fraction (fLF), occluded light fraction (oLF), and heavy fraction (HF) of soils under switchgrass and maize at 0–20 cm and 90–120 cm at the sandy (Michigan) and silty (Wisconsin) sites. Peaks at 2976–2898 and 2870–2839 cm^{-1} represent aliphatic (C–H stretch), 1550–1500 cm^{-1} for aromatic (C═C stretch), and 1660–1580 cm^{-1} for amide/quinone/ketone (C═O stretch), aromatic (C═C stretch), and carboxylate (C–O stretch) groups. Lower case letters represent a significant difference in peak area between switchgrass and maize at a given site, depth, and fraction at $\alpha = 0.05$.

Site	Depth (cm)	Vegetation	Aliphatic C			Aromatic C			Amide/quinone/ketone/aromatic/ carboxylate C		
			fLF	oLF	HF	fLF	oLF	HF	fLF	oLF	HF
Sandy	0–20 cm	Switchgrass	26.7(2.15)	31.1(1.76)	11.3(0.636)	23.0(1.09)	24.1(0.162)	22.0(1.56)	35.6(0.626)	43.4(0.856)	36.1(2.31)
		Maize	21.2(1.91)	27.9(1.06)	12.0(1.40)	22.0(0.860)	22.6(2.30)	20.7(0.398)	31.7(2.80)	38.4(3.71)	34.3(0.954)
	90–120 cm	Switchgrass	9.78^{a}(0.768)	10.2(1.40)	15.1(0.442)	20.0(1.14)	26.3(2.10)	37.2(3.83)	16.7(2.64)	21.0(3.06)	59.0(4.97)
		Maize	6.80^{b}(0.147)	12.5(2.66)	15.7(0.588)	20.6(1.54)	26.3(1.42)	28.3(1.92)	17.6(1.00)	27.5(5.43)	46.7(2.34)
Silty	0–20 cm	Switchgrass	25.4(2.78)	33.8(2.35)	12.5(0.807)	18.0(0.314)	21.8(1.37)	16.2(0.402)	31.6(1.45)	44.2(3.18)	30.7(0.795)
		Maize	24.8(1.11)	34.8(1.15)	12.2(1.03)	19.0(2.27)	22.7(0.688)	17.3(1.20)	36.1(3.44)	47.9(0.107)	31.6(1.58)
	90–120 cm	Switchgrass	11.2(0.177)	22.5(7.49)	10.4(1.02)	20.1(2.19)	20.4(4.90)	13.2(0.374)	19.9(2.59)	34.7(2.77)	25.7(1.38)
		Maize	12.4(1.08)	18.5(2.66)	10.8(1.20)	25.4(1.92)	19.5(2.30)	14.4(1.05)	23.7(2.01)	29.5(2.51)	27.8(0.380)

0–20 cm than at 90–120 cm in fLF and oLF for both sites (Table 2). Also, Δ^{14}C-CO_2 data demonstrate that microbial communities under switchgrass at 0–20 cm respired relatively young, recent photosynthates compared to those under maize at the sandy site (Fig. 2). These results indicate that switchgrass roots at shallow depth intervals increase the availability of recent plant-derived C, enhancing microbial respiration.

Plant growth and fresh C inputs into soil can accelerate the decomposition of SOC, a phenomenon referred to as the 'priming effect' (Löhnis 1926). Although our experiment was not designed to directly quantify the priming effect, we did not see clear evidence for the acceleration of SOC decomposition under switchgrass at our study sites. First, the bulk SOC concentration (Table 1, Fig. S1), as well as SOC stock and Δ^{14}C-SOC (Slessarev et al., in preparation), were similar under switchgrass and maize at both sites. Second, the Δ^{14}C-CO_2 data reveal that the major source of microbial respiration under switchgrass was recently fixed, plant-derived C, not older SOC at 0–20 cm (Fig. 2). For example, at the sandy site, the values of Δ^{14}C-CO_2 under switchgrass ranged between 20 and 25 ‰, while the values of Δ^{14}C-CO_2 under maize were between −82 and −47 ‰. The lower (i.e., older) value of Δ^{14}C-CO_2 (Fig. 2c) under maize than that under switchgrass suggests that maize, not switchgrass, could be depleting SOC. This is consistent with the report that microbes use different SOC pools for respiration dependent on vegetation types (shallow-rooted annual crops vs. switchgrass) (Szymanski et al., 2019). Third, the percent OC in HF was similar between switchgrass and maize at any depth intervals and sites (Table 1). While priming can occur in both particulate organic C and mineral-associated C (Olayemi et al., 2022; Zheng et al., 2023), a *meta*-analysis reveals that mineral-associated C experiences a more pronounced degree of positive priming (Zhang et al., 2022). Our results of similar percent of HF between switchgrass and maize, therefore, indicate that switchgrass and maize roots influenced mineral-associated OC to a similar degree. Taken together, growing deep-rooted switchgrass seems to have accelerated the magnitude of C fluxes, both in and out, of the soils via increased shallow root inputs and microbial respiration of that plant-derived C, with little priming of SOC at our study sites.

4.2. *Deep-rooted perennials supply aliphatic C into deep soil layers*

We hypothesized that deep-rooted perennials will increase the relative mass and OC of fLF and oLF, complex plant C to microbial C, and Δ^{14}C-SOC in each fraction (hypotheses 2 and 3); our results partially support this, in that switchgrass increased the relative OC and Δ^{14}C of fLF compared to maize at 90–120 cm (Fig. 3 and 7). These data indicate that switchgrass supplied new C inputs into deep soil layers, where maize roots did not reach. Previous studies also report that deep-rooted plants increased belowground C inputs (Weaver and Darland, 1949; Mclaughlin and Kszos, 2005; Slessarev et al., 2020). Expanding these findings, we found that deep-rooted perennials increased aliphatic C in

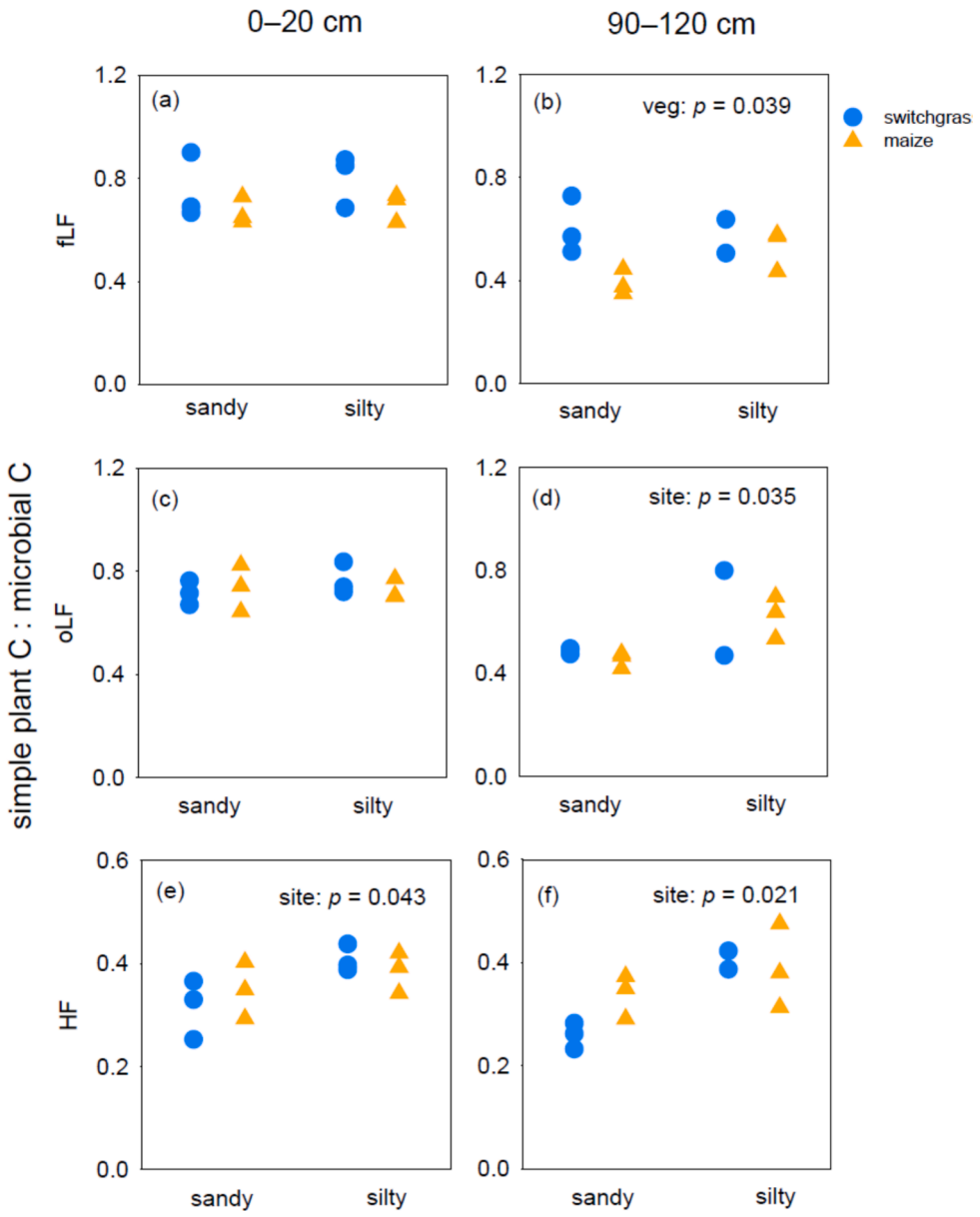

Fig. 5. Relative abundance of simple plant C to microbial C at 0–20 cm (left) and 90–120 cm (right) in free light fraction (fLF; a and b), occluded light fraction (oLF; c and d), and heavy fraction (HF; e and f) from two contrasting cropland sites planted with switchgrass (blue) or maize (orange) grown at the sandy (Kellogg Biological Station, MI) and silty (Arlington Agriculture Research Station) (N = 3). Simple plant C is aliphatic C = Σ(DRIFT peak height between 2976–2898 and 2870–2839 cm^{-1}). Microbial C is amide/quinone/keton/aromatic/carboxylate C = Σ(DRIFT peak height between 1660 and 1580 cm^{-1}).

fLF at 90–120 cm (Fig. 5.b). This type of C could be supplied as suberin (which is found in root cell walls), or organic acids that are common in root exudates (e.g., acetic, citric, oxalic, succinic acids) (Franke and Schreiber, 2007; Eshel and Beeckman, 2013; Vranova et al., 2013; Zhalnina et al., 2018; Williams and de Vries, 2020; Baker et al., 2024). Given the similar abundance of microbial C between switchgrass and maize while the greater abundance of simple plant C under switchgrass at 90–120 cm (Table 2, Fig. 5), it is likely that plant root inputs (e.g., dead root cells, border cells (previously called 'sloughed cells'), or root exudates) were the dominant type of C input that was enhanced under switchgrass at this depth.

Generally, different types of roots can impact SOC formation due to differences in biochemical traits, including C:N ratio, respiration rates, and root exudation. Low-order, distal roots exhibit relatively low C:N ratio and high respiration rates (Eshel and Beeckman, 2013; McCormack et al., 2015). Low-order roots can supply C into soil via relatively high root exudation rates and rapid turnover. In contrast, high-order roots occur in a higher branching hierarchy and transport water. While the rates of turnover and root exudation are relatively low for high-order roots, they can provide C to soil via border cells due to friction against mineral particles and slough-off. Recently, Wang et al. (2021) reported that low-order, absorptive roots enhance mineral-associated organic matter formation and SOC storage, while high-order, transport roots facilitate particulate organic matter formation. Similarly, our results could reflect the fact that deep switchgrass roots, which are presumably high-order roots optimized for water transport rather than nutrient acquisition and exudate production, contributed less to mineral SOC.

Our results have implications for managing agricultural land under climate change. First, deep-rooted perennials sequester and transfer more atmospheric C into soil than shallow-rooted annuals, as illustrated in the deeper and more abundant roots in switchgrass than in maize (Fig. 1). Although the overall changes in SOC concentration were marginal (Fig. S1), we demonstrate that deep-rooted perennials could bridge the interaction between the atmosphere and deeper soil layers and allow

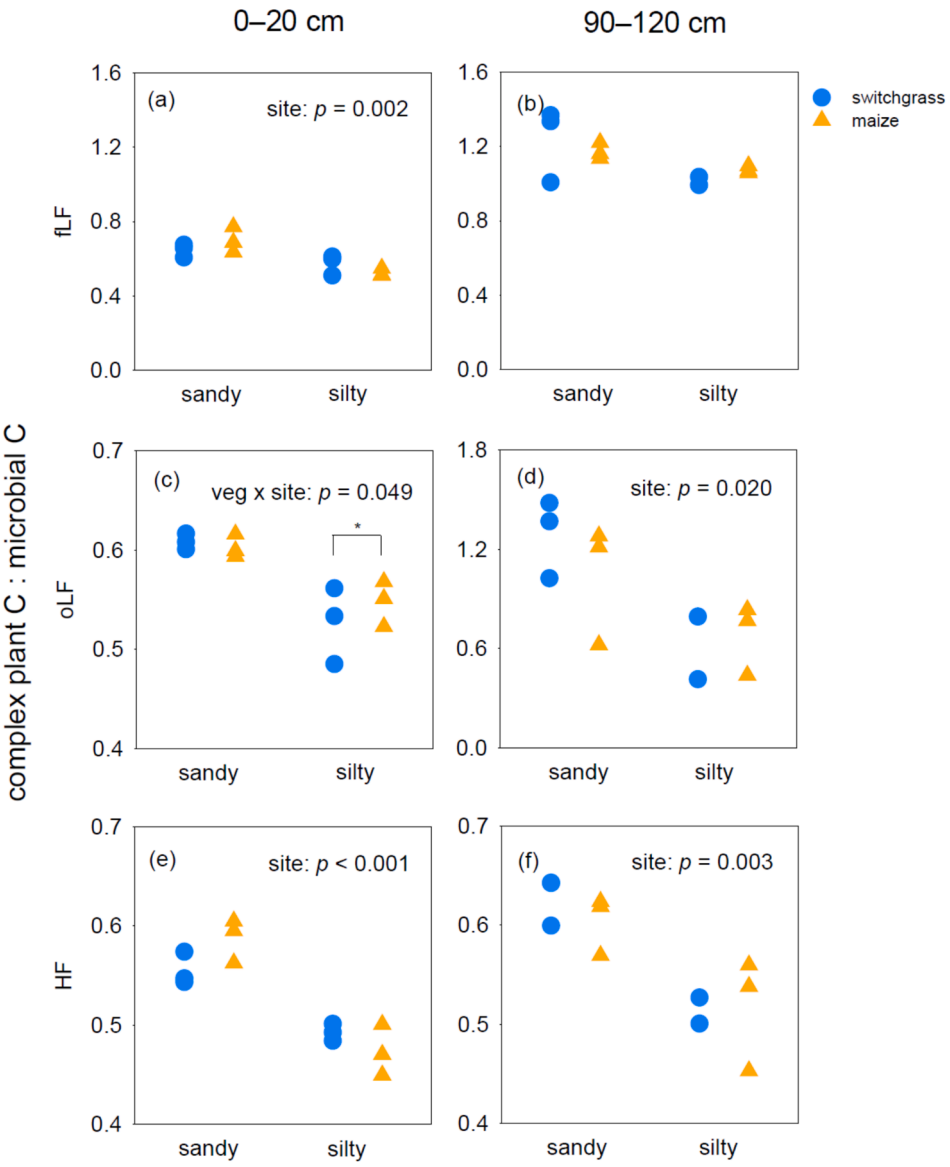

Fig. 6. Relative abundance of complex plant C to microbial C at 0–20 cm (left) and 90–120 cm (right) in free light fraction (fLF; a and b), occluded light fraction (oLF; c and d), and heavy fraction (HF; e and f) from two contrasting cropland sites planted with switchgrass (blue) or maize (orange) grown at the sandy (Kellogg Biological Station, MI) and silty (Arlington Agriculture Research Station) (N = 3). Complex plant C is aromatic C = Σ(DRIFT peak height between 1550 and 1500 cm^{-1}). Microbial C is amide/quinone/keton/aromatic/carboxylate C = Σ(DRIFT peak height between 1660 and 1580 cm^{-1}). Note the different scales on the y-axis for oLF.

atmospheric C to penetrate into the otherwise rarely tapped deep soil layers. Second, the newly added C entering soil under deep-rooted perennials appears to form relatively less-protected SOC at least on the time scales we measured. Increases in OC in fLF and Δ^{14}C-SOC in fLF (Figs. 3 and 7) indicate that the new, plant-added C is not associated with soil minerals that are thought to lead to long-term stabilization (Hicks-Pries et al. 2023). Third, our results demonstrate that combining density fractionation, DRIFT, and ^{14}C analyses can assess what type of C accrues in soil and identify which pools (e.g., mineral-associated or deep soils) accumulate C with management practices. This approach provides more mechanistic inference relative to previous studies that focused only on bulk SOC stocks or concentrations (Hungate et al., 1996; Garten and Wullschleger, 1999; Lajtha et al., 2014; Min et al., 2021). Ideally, future studies may employ multiple study sites, with varying cultivation histories and environmental conditions, to assess how growing deep-rooted perennials affects patterns of SOC properties in time or space.

4.3. *Density fractionation can only partially separate distinct SOC*

We used density fractionation to separate SOC into fLF, oLF, and HF. Notably we observed that the ^{14}C and DRIFT spectra provided mixed information about density fractions: relatively clear separation of DRIFT spectra (Fig. 4) vs. overlapped ^{14}C values among density fractions (Fig. 7). In our samples, mineral-associated OC (HF) contained peaks at 2,000–1,800 cm^{-1} due to quartz (Nguyen et al., 1991), which were not detected in particulate type OC (fLF and oLF) (Fig. 4). Also, the relative abundance of microbial C was greater in HF compared to fLF and oLF. These results support the traditional view that soil fractions fall along a spectrum of chemical characteristics and the origin of C from plant to microbes from fLF to oLF to HF (Golchin et al., 1994; Sollins et al., 2006; von Lützow et al., 2007). For example, alkyl C decreases but microbial products increase from fLF to oLF to HF (Golchin et al., 1994; Sollins et al., 2006; von Lützow et al., 2007).

The traditional view also argues that ^{14}C age increases from fLF to

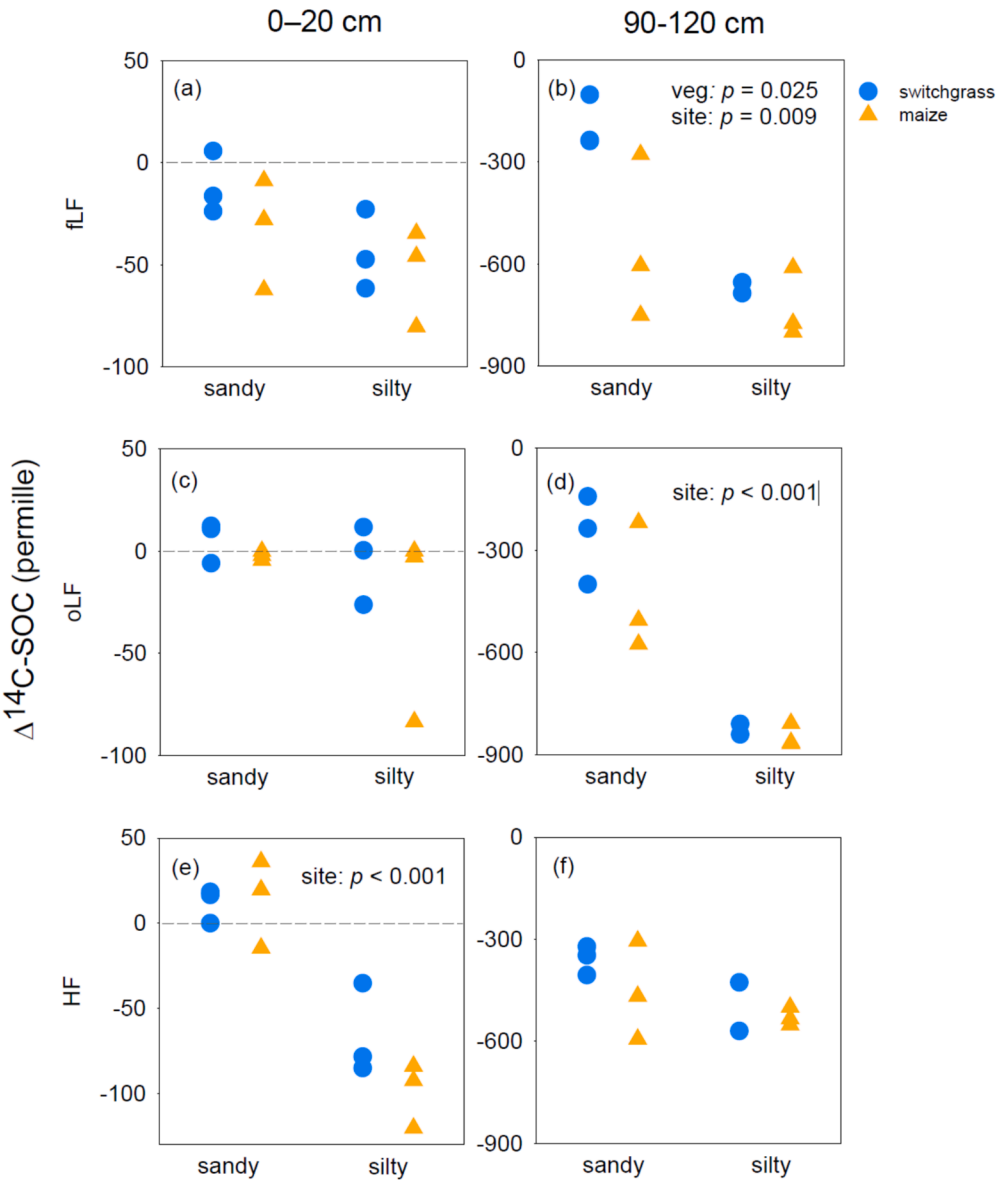

Fig. 7. $\Delta^{14}C$ of density fractionated soils ((fLF, free light fraction; oLF, occluded light fraction; HF, heavy fraction) under switchgrass (blue) and maize (orange) at 0–20 cm (left) and 90–120 cm (right) at the sandy and silty sites. Note the different scales on the y-axes. Dotted line represents modern C.

oLF to HF (Swanston et al., 2005; von Lützow et al., 2007; Heckman et al., 2022). However, we rarely observed a clear aging trend across the three density fractions (Fig. 7). For example, $\Delta^{14}C$ values of fLF were more negative than those of HF at 90–120 cm at both sandy and silty sites, demonstrating that fLF can contain aged SOC. Consistent with our results, a growing body of evidence suggests that multiple, non-linear pathways can lead to SOC formation. For example, some studies reported overlapped ^{14}C age among fractions (Trumbore and Zheng, 1996; Crow et al., 2009), suggesting that different fractions do not necessarily form in a linear fashion. Hall et al. (2020) demonstrated that lignin, one of the major components of fLF, can be preserved in long-lasting soil particles due to its chemical complexity. After comparing 156 soil samples collected across the National Ecological Observatory Network, Yu et al. (2022) reported that particulate and mineral-associated OC can exhibit similar isotopic and DRIFT spectra. Combined, these results, including ours, suggest that the physical properties of soil (e.g., density, particle size) can decouple from the chemical properties of soil C, and that equating physical or chemical fractions to the persistent SOC requires some caution, particularly in the context of different rooting systems.

5. Conclusions

Integrating climate-smart practices for both soil health and carbon sequestration is a key challenge for managing agricultural lands. We utilized density fractionation, DRIFT, and ^{14}C analyses to explore the effects of deep-rooted perennials on microbial respiration and SOC properties. In addition to increasing root C, we demonstrate that microbial communities under deep-rooted perennials respire plant-derived C from shallow soil layers, and that growing deep-rooted perennials can increase aliphatic C inputs into fLF at depth. Also, our results highlight that while fLF, oLF, and HF exhibit distinct DRIFT spectra, the $\Delta^{14}C$ values of these fractions can be similar. Together, this study illustrates that deep-rooted perennials may influence the formation and persistence of new SOC along the depth profile by altering C inputs and microbial activity.

Author contributions

KM (Kyungjin Min), ES, EO, KM (Karis McFarlane), JP, AB, EN, GS and KT designed the experiment. KM (Kyungjin Min), ES, MK, KM (Karis

McFarlane), AJ, and EN performed the experiment. KM (Kyungjin Min) and ES analyzed the data. KM (Kyungjin Min) wrote the first draft of the manuscript. All authors contributed substantially to the data interpretation and gave final approval for the submission of manuscript.

CRediT authorship contribution statement

Kyungjin Min: Writing – review & editing, Writing – original draft, Investigation, Funding acquisition, Formal analysis, Data curation, Conceptualization. **Erin Nuccio:** Writing – review & editing, Supervision, Project administration, Investigation, Funding acquisition. **Eric Slessarev:** Writing – review & editing, Investigation. **Megan Kan:** Writing – review & editing, Data curation. **Karis J. McFarlane:** Writing – review & editing, Investigation. **Erik Oerter:** Writing – review & editing, Investigation. **Anna Jurusik:** Writing – review & editing, Visualization. **Gregg Sanford:** Conceptualization, Writing – review & editing. **Kurt D Thelen:** Conceptualization, Writing – review & editing. **Jennifer Pett-Ridge:** Writing – review & editing, Investigation, Data curation. **Asmeret Asefaw Berhe:** Writing – review & editing.

Declaration of competing interest

We declare no competing financial interests that could have appeared to influence the work reported in this article.

Acknowledgments

We thank Dr. Phillip Robertson at Michigan State University, and Dr. Randy Jackson and Dr. Gregg Sanford at the University of Wisconsin-Madison for allowing us to collect soil samples in their long-term experimental field sites. This work was supported by Lawrence Livermore National Laboratory (LLNL)'s Lab Directed Research and Development program (#19-ERD-010) and a DOE Early Career Research Program award to EN (SCW1711). Additional support for KM was provided by the Technology Development Project for Creation and Management of Ecosystem based Carbon Sinks through KEITI, Ministry of Environment, Korea (RS-2023-00218237), the National Research Foundation of Korea grant funded by the Korea government (RS-2024-00336378, RS-2024-00405420, RS-2024-00398300), and the University of California Merced Chancellor's Fellowship. Site support for maintenance of long-term plots in MI and WI was provided by the Great Lakes Bioenergy Research Center, U.S. Department of Energy, Office of Science, Biological and Environmental Research Program under Award Number (DE-SC0018409), the National Science Foundation Long-term Ecological Research Program (DEB 2224712) at the Kellogg Biological Station, and by Michigan State University AgBioResearch. Support for Dr. Sanford was provided by USDA NIFA grant (2024-67019-42335) and USDA SARE grant (H009987615). We thank the Imaging and Microscopy Facility at UC Merced (director: Kennedy Nguyen, Ph.D.) for help with scanning electron microscopy. Work at LLNL was conducted under the auspices of the Department of Energy Contract DE-AC52-07NA27344.

Appendix A. Supplementary data

Supplementary data to this article can be found online at https://doi.org/10.1016/j.geoderma.2025.117202.

Data availability

Data will be made available on request.

References

Angst, G., John, S., Mueller, C.W., Kögel-Knabner, I., Rethemeyer, J., 2016. Tracing the sources and spatial distribution of organic carbon in subsoils using a multibiomarker approach. Sci. Rep. 6, 29478.

Angst, G., Mueller, K.E., Nierop, K.G., Simpson, M.J., 2021. Plant- or microbial-derived? A review on the molecular composition of stabilized soil organic matter. Soil Biol. Biochem. 156, 108189. https://doi.org/10.1016/j.soilbio.2021.108189.

Baker, N.R., Zhalnina, K., Yuan, M., Herman, D., Ceja-Navarro, J.A., Sasse, J., Jordan, J. S., Bowen, B.P., Wu, L., Fossum, C., Chew, A., Fu, Y., Saha, M., Zhou, J., Pett-Ridge, J., Northen, T.R., Firestone, M., 2024. Nutrient and moisutre limitations reveal keystone metabolites linking rhizosphere metabolomes and microbiomes. Proc. Natl. Acad. Sci. 121(32), E2303439121.

Broek, T.A.B., Ognibene, T.J., McFarlane, K.J., Moreland, K.C., Brown, T.A., Bench, G., 2021. Conversion of the LLNL/CAMS 1 MV biomedical AMS system to a semi-automated natural abundance 14C spectrometer: system optimization and performance evaluation. Nucl. Instrum. Methods Phys. Res. Sect. B 499, 124–132. https://doi.org/10.1016/j.nimb.2021.01.022.

Button, E.S., Pett-Ridge, J., Murphy, D.V., Kuzyakov, Y., Chadwick, D.R., Jones, D.L., 2022. Deep-C storage: biological, chemical and physical strategies to enhance carbon stocks in agricultural subsoils. Soil Biol. Biochem. 170, 108697. https://doi.org/10.1016/j.soilbio.2022.108697.

Conant, R.T., Cerri, C.E.P., Osborne, B.B., Paustian, K., 2017. Grassland management impacts on soil carbon stocks: a new synthesis. Ecol. Appl. 27, 662–668. https://doi.org/10.1002/eap.1473.

Crow, S.E., Lajtha, K., Filley, T., Swanston, C., Bowden, R., Caldwell, B.A., 2009. Sources of plant-derived carbon and stability of organic matter in soil: implications for global change. Glob. Chang. Biol. 15, 2003–2019.

Dijkstra, F.A., Zhu, B., Cheng, W., 2021. Root effects on soil organic carbon: a double-edged sword. New Phytol. 230, 60–65. https://doi.org/10.1111/nph.17082.

Driouich, A., Follet-Gueye, M., Vicre-Gibouin, M., Hawes, M., 2013. Root border cells and secretions as critical elements in plant host defense. Curr. Opin. Plant Biol. 16, 489–495.

Ellerbrock, R.H., Gerke, H.H., 2004. Characterizing organic matter of soil aggregate coatings and biopores by Fourier transform infrared spectroscopy. Eur. J. Soil Sci. 55, 219–228.

Eshel, A., Beeckman, T., 2013. Plant Roots: The Hidden Half. CRC Press.

Fisher, M.J., Rao, I.M., Ayarza, M.A., Lascano, C.E., Sanz, J.I., Thomas, R.J., Vera, R.R., 1994. Carbon storage by introduced deep-rooted grasses in the South American savannas. Nature 371, 236–238. https://doi.org/10.1038/371236a0.

Franke, R., Schreiber, L., 2007. Suberin – a biopolyester forming apoplastic plant interfaces. Curr. Opin. Plant Biol. 10, 252–259. https://doi.org/10.1016/j.pbi.2007.04.004.

Franzluebbers, A.J., 1999. Microbial activity in response to water-filled pore space of variably eroded southern Piedmont soils. Appl. Soil Ecol. 11, 91–101.

Garten, C.T., Wullschleger, S.D., 1999. Soil carbon inventories under a bioenergy crop (switchgrass): measurement limitations. J. Environ. Qual. 28, 1359–1365. https://doi.org/10.2134/jeq1999.00472425002800040041x.

Golchin, A., Oades, J.M., Skjemstad, J.O., Clarke, P., 1994. Study of free and occulded particulate organic mater in soils by solid state ^{13}C CP/MAS NMR spectroscopy and scanning electron microscopy. Aust. J. Soil Res. 32, 285–309.

Haichar, F.Z., Santaella, C., Heulin, T., Achouak, W., 2014. Root exudates mediated interactions belowground. Soil Biol. Biochem. 77, 69–80.

Hall, S.J., Ye, C., Weintraub, S.R., Hockaday, W.C., 2020. Molecular trade-offs in soil organic carbon composition at continental scale. Nat. Geosci. 13, 687–692.

Heckman, K., Hicks-Pries, C., Lawrence, C.R., Rasmussen, C., Crow, S.E., Hoyt, A.M., von Fromm, S.F., Shi, Z., Stoner, S., McGrath, C., Bemm-Miller, J., Berhe, A.A., Blankinship, J.C., Keiluweit, M., Marin-Spiotta, E., Monroe, G., Plante, A.F., Schimel, J., Sierra, C.A., Thompson, A., Wagai, R., 2022. Beyond bulk: density fractions explain heterogeneity in global soil carbon abundance and persistence. Glob. Chang. Biol. 28, 1178–1196.

Hicks-Pries, C., Ryals, R., Zhu, B., Min, K., Cooper, A., Goldsmith, S., Pett-Ridge, J., Torn, M., Berhe, A., 2023. The deep soil organic carbon response to global change. Annu. Rev. Ecol. Evol. Syst. 54, 375–401. https://doi.org/10.1146/annurev-ecolsys-102320-085332.

Hungate, B., Jackson, R., Field, C., Chapin, F., Sciences, B., 1996. Detecting changes in soil carbon in CO2 enrichment experiments. Plant Soil 187, 135–145.

Keiluweit, M., Bougoure, J.J., Nico, P.S., Pett-Ridge, J., Weber, P.K., Kleber, M., 2015. Mineral protection of soil carbon counteracted by root exudates. Nat. Clim. Chang. 5, 588–595. https://doi.org/10.1038/nclimate2580.

Kell, D.B., 2011. Breeding crop plants with deep roots: their role in sustainable carbon, nutrient and water sequestration. Ann. Bot. 108, 407–418. https://doi.org/10.1093/aob/mcr175.

Kell, D.B., 2012. Large-scale sequestration of atmospheric carbon via plant roots in natural and agricultural ecosystems: why and how. Philos. Trans. R. Soc. B 367, 1589–1597. https://doi.org/10.1098/rstb.2011.0244.

Lajtha, K., Bowden, R.D., Nadelhoffer, K., 2014. Litter and root manipulations provide insights into soil organic matter dynamics and stability. Soil Sci. Soc. Am. J. 78, S261–S269. https://doi.org/10.2136/sssaj2013.08.0370nafsc.

Lal, R., 2004. Soil carbon sequestration to mitigate climate change. Geoderma 123, 1–22. https://doi.org/10.1016/j.geoderma.2004.01.032.

Löhnis, F., 1926. Nitrogen availability of green manures. Soil Sci. 12, 253–290.

Longbottom, T., Wahab, L., Min, K., Jurusik, A., Moreland, K., Dolui, M., Thao, T., Gonzales, M., Perez-Rojas, Y., Alvarez, J., Malone, Z., Ghezzehei, T., Berhe, A., 2022. What's soil got to do with climate change? GSA Today 32, 4–10. https://doi.org/10.1130/GSATG519A.1.

Lorenz, K., Lal, R., 2005. The depth distribution of soil organic carbon in relation to land use and management and the potential of carbon sequestration in subsoil horizons. Adv. Agron. 88, 35–66. https://doi.org/10.1016/S0065-2113(05)88002-2.
Mainka, M., Summerauer, L., Wasner, D., Garland, G., Griepentrog, M., Berhe, A.A., Doetterl, S., 2022. Soil geochemistry as a driver of soil organic matter composition: Insights from a soil chronosequence. Biogeosciences 19, 1675–1689. https://doi.org/10.5194/bg-19-1675-2022.
McCormack, M.L., Dickie, I.A., Eissenstat, D.M., Fahey, T.J., Fernandez, C.W., Guo, D., Erik, A., Iversen, C.M., Jackson, R.B., Helmisaari, H.S., Hobbie, E.A., Iversen, C.M., Jackson, R.B., Leppälammi-Kujansuu, J., Norby, R.J., Phillips, R.P., Pregitzer, K.S., Pritchard, S.G., Rewald, B., Zadworny, M., 2015. Redefining fine roots improves understanding of below-ground contributions to terrestrial biosphere processes. New Phytol. 207, 505–518. https://doi.org/10.1111/nph.13363.
Mclaughlin, S., Kszos, L.A., 2005. Development of switchgrass (Panicum virgatum) as a bioenergy feedstock in the United States. Biomass Bioenergy 28, 515–535. https://doi.org/10.1016/j.biombioe.2004.05.006.
Miao, Y., Lv, J., Huang, H., Cao, D., Zhang, S., 2020. Molecular characterization of root exudates using Fourier Transform Ion Cyclotron Resonance Mass Spectrometry. J. Environ. Sci. 98, 22–30.
Miltner, A., Bombach, P., Schmidt-Brücken, B., Kästner, M., 2012. SOM genesis: microbial biomass as a significant source. Biogeochemistry 111, 41–55. https://doi.org/10.1007/s10533-011-9658-z.
Min, K., Choi, M., 2022. Resource landscape, microbial activity, and community composition under wintering crane activities in the Demilitarized Zone, South Korea. Plos ONE 17, e0268461. https://doi.org/10.1371/journal.pone.0268461.
Min, K., Slessarev, E., Kan, M., McFarlane, K., Oerter, E., Pett-Ridge, J., Nuccio, E., Berhe, A.A., 2021. Active microbial biomass decreases, but microbial growth potential remains similar across soil depth profiles under deeply- vs. shallow-rooted plants. Soil Biol. Biochem. 162, 108401. https://doi.org/10.1016/j.soilbio.2021.108401.
Nguyen, T.T., Janik, L.J., Raupach, M., 1991. Diffuse reflectance infrared fourier transform (DRIFT) spectroscopy in soil studies. Aust. J. Soil Res. 29, 49–67.
Olayemi, O.P., Kallenbach, C.M., Wallenstein, M.D., 2022. Distribution of soil organic matter fractions are altered with soil priming. Soil Biol. Biochem. 164, 108494. https://doi.org/10.1016/j.soilbio.2021.108494.
Paustian, K., Lehmann, J., Ogle, S., Reay, D., Robertson, G.P., Smith, P., 2016. Climate-smart soils. Nature 532, 49–57. https://doi.org/10.1038/nature17174.
Peixoto, L., Elsgaard, L., Rasmussen, J., Kuzyakov, Y., Banfield, C., Dippold, M., Olesen, J., 2020. Decreased rhizodeposition, but increased microbial carbon stabilization with soil depth down to 3.6 m. Soil Biol. Biochem. 150, 108008.
Pett-Ridge, J., Shi, S., Estera-Molina, K., Nuccio, E., Yuan, M., Rijkers, R., Swenson, T., Zhalnina, K., Northen, T., Zhou, J., Firestone, M.K., 2020. Rhizosphere carbon turnover from cradle to grave: the role of microbe-plant interactions. In: Gupta, V.V. S., Sharma, A.K Springer (Eds.), Rhizosphere Biology: Interactions between Microbes and Plants. https://doi.org/10.1007/978-981-15-6125-2_2#DOI.
R Core Team, 2024. R: A language and environment for statistical computing. R foundation for statistical computing, Vienna, Austria. www.R-project.org.
Rasse, D., Rumpel, C., Dignac, M., 2005. Is soil carbon mostly root carbon? Mechanisms for a specific stabilization. Plant Soil 269, 341–356.
Riederer, M., Matzke, K., Ziegler, F., Kögel-Knabner, I., 1993. Occurrence, distribution, and fate of the lipid plant biopolymers cutin and suberin in temperate forest soils. Soil Biol. Biochem. 20, 1063–1076.
Ryals, R., Kaiser, M., Torn, M., Berhe, A.A., Silver, W.L., 2014. Impacts of organic matter amendments on carbon and nitrogen dynamics in grassland soils. Soil Biol. Biochem. 68, 52–61.
Sanderman, J., Hengl, T., Fiske, G.J., 2017. Soil carbon debt of 12,000 years of human land use. PNAS 115, E1700. https://doi.org/10.1073/pnas.1800925115.
Sanderman, J., Hengl, T., Fiske, G.J., 2018. Correction for Sanmderman et al. 2017. Soil carbon debt of 12,000 years of human land use. Proc. Natl. Acad. Sci. U.S.A. 115, E1700. https://doi.org/10.1073/pnas.1800925115.
Schiedung, M., Tregurtha, C.S., Beare, M.H., Thomas, S.M., Don, A., 2019. Deep soil flipping increases carbon stocks of New Zealand grasslands. Glob. Chang. Biol. 25, 2296–2309. https://doi.org/10.1111/gcb.14588.
Shahzad, T., Rashid, M.M.I.M., Maire, V., Barot, S., Perveen, N., Alvarez, G., Mougin, C., Fontaine, S., 2018. Root penetration in deep soil layers stimulates mineralization of millennia-old organic carbon. Soil Biol. Biochem. 124, 150–160. https://doi.org/10.1016/j.soilbio.2018.06.010.
Slessarev, E.W., Nuccio, E.E., McFarlane, K.J., Ramon, C.E., Saha, M., Firestone, M.K., Pett-Ridge, J., 2020. Quantifying the effects of switchgrass (Panicum virgatum) on deep organic C stocks using natural abundance ^{14}C in three marginal soils. GCB Bioenergy 12, 1–14. https://doi.org/10.1111/gcbb.12729.
Sokol, N.W., Bradford, M.A., 2019. Microbial formation of stable soil carbon is more efficient from belowground than aboveground input. Nat. Geosci. 12, 46–53. https://doi.org/10.1038/s41561-018-0258-6.
Sokol, N.W., Slessarev, E., Marchmann, G.L., Nicolas, A., Blazewicz, S.J., Brodie, E.L., Firestone, M.K., Foley, M.M., Hestrin, R., Hungate, B.A., Koch, B.J., Stone, B.W., Sullivan, M.B., Zablocki, O., LLNL Soil Microbiome Consortium, Pett-Ridge, J., 2022. Life and death in the soil microbiome: how ecological processes influence biogeoghemistry. Nat. Rev. Microbiol. 20, 415–430. https://doi.org/10.1038/s41579-022-00695-z.
Sollins, P., Swanston, C., Kleber, M., Filley, T., Kramer, M., Crow, S., Caldwell, B.A., Lajtha, K., Bowden, R., 2006. Organic C and N stabilization in a forest soil: evidence from sequential density fractionation. Soil Biol. Biochem. 38, 3313–3324.
Spielvogel, S., Prietzel, J., Kögel-Knabner, I., 2010. Lignin phenols and cutin-and suberin-derived aliphatic monomers as biomarkers for stand history, SOM source, and turnover. World Cong. Soil Sci. 74–77.
Stuiver, M., Polach, H., 1977. Discussion reporting of ^{14}C data. Radiocarbon 19, 355–363.
Swanston, C.W., Torn, M.S., Hanson, P.J., Southon, J.R., Garten, C.T., Hanlon, E.M., Ganio, L., 2005. Initial characterization of processes of soil carbon stabilization using forest stand-level radiocarbon enrichment. Geoderma 128, 52–62. https://doi.org/10.1016/j.geoderma.2004.12.015.
Szymanski, L.M., Sanford, G.R., Heckman, K.A., Jackson, R.D., Marin-Spiotta, E., 2019. Conversion to bioenergy crops alters the amount and age of microbially-respired soil carbon. Soil Biol. Biochem. 128, 35–44.
Trumbore, S.E., Zheng, S., 1996. Comparison of fractionation methods for soil organic matter ^{14}C analysis. Radiocarbon 38, 219–229.
Tückmantel, T., Leuschner, C., Preusser, S., Kandeler, E., Angst, G., Mueller, C.W., Meier, I.C., 2017. Root exudation patterns in a beech forest: dependence on soil depth, root morphology, and environment. Soil Biol. Biochem. 107, 188–197. https://doi.org/10.1016/j.soilbio.2017.01.006.
von Lützow, M., Kögel-Knabner, I., Ekschmitt, K., Flessa, H., Guggenberger, G., Matzner, E., Marschner, B., 2007. Soil Biol. Biochem. 39, 2183–2207.
Vranova, V., Rejsek, K., Formanek, P., 2013. Aliphatic, cyclic, and aromatic organic acids, vitamins, and carbohydrates in soil: a review. Scientific World J.
Waksman, S.A., 1925. What is humus? Proc. Natl. Acad. Sci. 11, 463–468. https://doi.org/10.1073/pnas.11.8.463.
Wang, Q., Zhang, Z., Guo, W., Zhu, X., Xiao, J., Liu, Q., Yin, H., 2021. Absorptive and transport roots differ in terms of their impacts on rhizosphere soil carbon storage and stability in alpine forests. Soil Biol. Biochem. 161, 108379. https://doi.org/10.1016/j.soilbio.2021.108379.
Weaver, J.E., Darland, R.W.R., 1949. Soil-root relationships of certain native grasses in various soil types. Ecol. Monogr. 19, 303–338. https://doi.org/10.2307/1943273.
Williams, A., de Vries, F.T., 2020. Plant root exudation under drought: implications for ecosystem functioning. New Phytol. 225, 1899–1905. https://doi.org/10.1111/nph.16223.
Yu, W., Huang, W., Weintraub-Leff, S.R., Hall, S.J., 2022. Where and why do particulate organic matter (POM) and mineral-associated organic matter (MAOM) differ among diverse soils? Soil Biol. Biochem. 172, 108756. https://doi.org/10.1016/j.soilbio.2022.108756.
Zhalnina, K., Louie, K.B., Hao, Z., Mansoori, N., da Rocha, U.N., Shi, S., Cho, H., Karaoz, U., Loque, D., Bowen, B.P., Firestone, M.K., Northen, T.R., Brodie, E.L., 2018. Dynamic root exudate chemistry and microbial substrate preferences drive patterns in rhizosphere microbial community assembly. Nat. Microbiol. 3, 470–480. https://doi.org/10.1038/s41564-018-0129-3.
Zhang, F., Chen, X., Yao, S., Ye, Y., Zhang, B., 2022. Responses of soil mineral-associated and particulate organic carbon to carbon input: a meta-analysis. Sci. Total Environ. 829, 154626. https://doi.org/10.1016/j.scitotenv.2022.154626.
Zheng, Y., Jin, J., Wang, X., Clark, G., Franks, A., Tang, C., 2023. Nitrogen addition increases the glucose-induced priming effect of the particulate but not the mineral-associated organic carbon fraction. Soil Biol. Biochem. 184, 109106. https://doi.org/10.1016/j.soilbio.2023.109106.